Rotation of a Bose-Einstein condensate held under a toroidal trap

Amandine Aftalion and Peter Mason
Ecole Polytechnique, CMAP, UMR-CNRS 7198, F-91128 Palaiseau cedex, France
(Received 4 November 2009; published 11 February 2010)

The aim of this paper is to perform a numerical and analytical study of a rotating Bose-Einstein condensate placed in a harmonic plus Gaussian trap, following the experiments of Bretin *et al.* [Phys. Rev. Lett. **92**, 5 (2004)]. The rotational frequency Ω has to stay below the trapping frequency ω of the harmonic potential and we find that the condensate has an annular shape containing a triangular vortex lattice. As Ω approaches ω, the width of the condensate and the circulation inside the central hole get large. We are able to provide analytical estimates of the size of the condensate and the circulation both in the lowest Landau level limit and in the Thomas-Fermi limit, providing an analysis that is consistent with experiment.

DOI: 10.1103/PhysRevA.81.023607 PACS number(s): 03.75.Hh, 05.30.Jp, 74.25.Uv

I. INTRODUCTION

The investigation of rotating gases or liquids is a central issue in the theory of superfluidity since they give rise to quantized vortices [1,2]. During recent years, several experiments using rotating atomic Bose-Einstein condensates have led to the observation of vortices. These condensates are usually confined in a harmonic potential with cylindrical symmetry around the rotation axis z. Two limiting regimes occur depending on the ratio of the rotation frequency Ω and the trap frequency ω in the xy plane. When Ω is notably smaller than ω, only one or a few vortices are present at equilibrium [3,4]. A Thomas-Fermi analysis can be performed to analyze this regime because the coupling constant describing the interactions is often large in the experiments [5,6]. When Ω approaches ω, since the centrifugal force nearly balances the trapping force, the radius of the rotating gas increases, and the vortices arrange themselves on a triangular lattice [7–10]. A new class of phenomena in this regime of fast rotation is predicted in relation with quantum Hall physics [6,11–17]. Indeed the one-body Hamiltonian written in the rotating frame is similar to that of a charged particle in a uniform magnetic field and one can use the Landau levels structure to analyze the ground state of the condensate and describe the properties of the lattice.

In order to analyze the regime of fast rotation, one approach consists in adding a quartic potential to the harmonic potential. For this type of potential, the trapping force is always greater than the centrifugal force so that the regime $\Omega > \omega$ can be explored. The condensate is then seen to exhibit a more complex structure with regards to its density distribution and the arrangement of vortices [17–24]. In particular, a multiply quantized vortex, or giant vortex, appears for large values of the rotational frequency Ω and the condensate is located within a thin annulus [21]. When Ω is decreased from this situation, a circle of vortices exists inside the condensate [22].

A number of experiments have been performed in which a laser beam is shone into an otherwise harmonically trapped condensate [25–28], thus creating a trapping potential of the form harmonic plus Gaussian. Often in experiments, the laser beam is weak and hence the Gaussian term is small and for the purpose of analysis can be expanded so that the resulting potential can be approximated by a harmonic plus quartic potential. A different approach to analyzing these experiments is to consider the full harmonic plus Gaussian trapping potential.

The aim of this paper is to perform a numerical and analytical study of a rotating condensate placed in a harmonic plus Gaussian trap as in the experiment of Refs. [25,26]. The specific feature of the Gaussian potential with respect to the quartic one is that the rotation frequency Ω cannot get arbitrarily large but stays below ω, the trapping frequency of the harmonic potential. We will show that, according to the parameters of the system, the condensate can either be a disk or an annulus. Furthermore, we will show that as Ω approaches ω, the condensate always expands to become a large annulus with a vortex lattice inside the condensate and a large circulation within the central hole. This is in contrast to the harmonic plus quartic trap, which develops a giant vortex and a thin annulus. Using the lowest Landau level (LLL) states, we will give an analytical description of the phenomena seen numerically. We estimate the radii R_1 and R_2 of the condensate and the circulation around the inside hole. The circulation is of order $R_1 R_2$ and thus is much bigger than that given by a uniform lattice (which would be R_1^2).

This paper is organized as follows. Section II contains a brief formalisation of the problem, introducing the energy functional followed by various numerical observations in Sec. III. The lowest Landau level analysis for the regime Ω close to ω is presented in Sec. IV, which provides the main analytical results of the paper. Finally, Sec. V is devoted to extra computations in the Thomas-Fermi regime.

II. FORMULATION

A two-dimensional Bose-Einstein condensate trapped at absolute zero temperature can be described by a macroscopic condensate wave function (order parameter) Ψ. The ground state of the rotating system is determined by minimizing the energy functional $E' = E - \Omega L_z$ where $L_z = \Psi^*[\hat{z} \cdot (\boldsymbol{r} \times \boldsymbol{p})]\Psi$ is the z component of angular momentum along the rotation axis (for linear momentum $\boldsymbol{p}$). The energy functional, in the frame rotating with angular velocity Ω, is then

$$E' = \int_{\mathcal{V}} \left[\frac{\hbar^2}{2m} |\nabla \Psi|^2 + V_{\mathrm{tr}}(r)|\Psi|^2 + \frac{U_0}{2}|\Psi|^4 - \Omega L_z \right] dV, \tag{1}$$

with $r^2 = x^2 + y^2$ and where the integral is carried out over the spatial domain $\mathcal{V}$. The trapping potential is composed of a harmonic plus Gaussian term,

$$V_{\rm tr} = V_0 \exp\left(-2r^2/w_0^2\right) + \tfrac{1}{2}m\omega^2 r^2. \quad (2)$$

When the atoms are assumed to occupy the ground state of the harmonic oscillator in the z direction, with energy $\hbar\omega_z/2$ and extension $a_z = \sqrt{\hbar/m\omega_z}$, suppression of the condensate in the z direction is allowed provided the characteristic energy $\hbar\omega_z$ is very large in comparison with the other energy scales. Here ω_z is the frequency of the confinement in the z direction. The two-dimensional coupling parameter is then $U_0 = \sqrt{8\pi}\hbar^2 a_s N/ma_z$ for N identical atoms with s-wave scatting length a_s [17].

The system can be nondimensionalised by choosing ω, $\hbar\omega$, and $\sqrt{\hbar/(m\omega)}$ as units of frequency, energy, and length, respectively. Thus, on defining a nondimensional coupling parameter $g = mU_0/\hbar^2$, the energy functional takes the nondimensionalized form

$$E' = \int_{\mathcal{V}} \left[\frac{1}{2}|\nabla\psi|^2 + V(r)|\psi|^2 + \frac{g}{2}|\psi|^4 - \Omega L_z\right] dV, \quad (3)$$

for external toroidal potential trap

$$V(r) = Ae^{-l^2r^2} + \tfrac{1}{2}r^2, \quad (4)$$

with $A = V_0/\hbar\omega$ and inverse waist $l = (2\hbar/m\omega w_0^2)^{1/2}$. The energy functional (3) is subject to the normalization

$$\int_{\mathcal{V}} |\psi|^2 r\, dV = 1. \quad (5)$$

In this scaling, large rotation implies that Ω gets close to 1. Note that in experiments l is often small so that the potential $V(r)$ in Eq. (4) can be expanded to give

$$V(r) \sim \tfrac{1}{2}(1 - 2Al^2)r^2 + \tfrac{1}{2}Al^4r^4, \quad (6)$$

from which a critical frequency around $1 - 2Al^2$ is observed [21]. However, in this paper we retain the toroidal potential given by Eq. (4) for the numerical and analytical analysis.

We will perform a full numerical analysis of the experimental case of [25], which will lead us to a numerical and analytical description of several model cases which prove to be different from the harmonic plus quartic trap considered in [21,22]. In particular, as Ω gets close to 1, the condensate has an annular shape, its width always becomes large, and a vortex lattice is present with a circulation inside the annulus. We are able to estimate these various quantities.

III. NUMERICAL OBSERVATIONS

A. The effective potential

When the condensate is put into rotation, the effective trapping potential to be considered is not given by Eq. (4) but is instead given by

$$V_{\rm eff} = V(r) - \tfrac{1}{2}\Omega^2 r^2. \quad (7)$$

Therefore according to the values of A, l, and Ω, this effective potential can produce either a disk condensate or an annular condensate. To see this, notice first that the effective potential (7) has a minimum that occurs for $r = r_0 \geqslant 0$ given by

$$r_0^2 = \frac{1}{l^2}\log\left(\frac{2Al^2}{1-\Omega^2}\right), \quad (8)$$

provided

$$q \equiv \frac{2Al^2}{1-\Omega^2} \geqslant 1. \quad (9)$$

If $q \geqslant 1$, the effective potential has a local minimum and it can lead to two different situations: Either the condensate is a disk or an annulus. For existence of an inner boundary, we must have $q \geqslant 1 + \delta$ for some positive (not necessarily small) δ. As $\Omega \to 1$, $q \geqslant 1 + \delta$ is always satisfied and so an inner boundary is created. The determination of the value of δ is not readily obtained as it depends on the normalization condition (5). Conversely, if $q < 1$, then the condensate is always a disk.

Figure 1 shows three examples of the effective potential (7) plotted against radial distance from the center of the condensate along constant θ for the parameters $\{g, A, l\} = \{100, 25, 0.03\}$, $\{1000, 10, 0.75\}$, and $\{500, 100, 0.9\}$, with $\Omega = 0$. In the first parameter set $q < 1$, the condensate is a disk and the density maximum is at the center. In the second parameter set, there is a local density minimum at the center

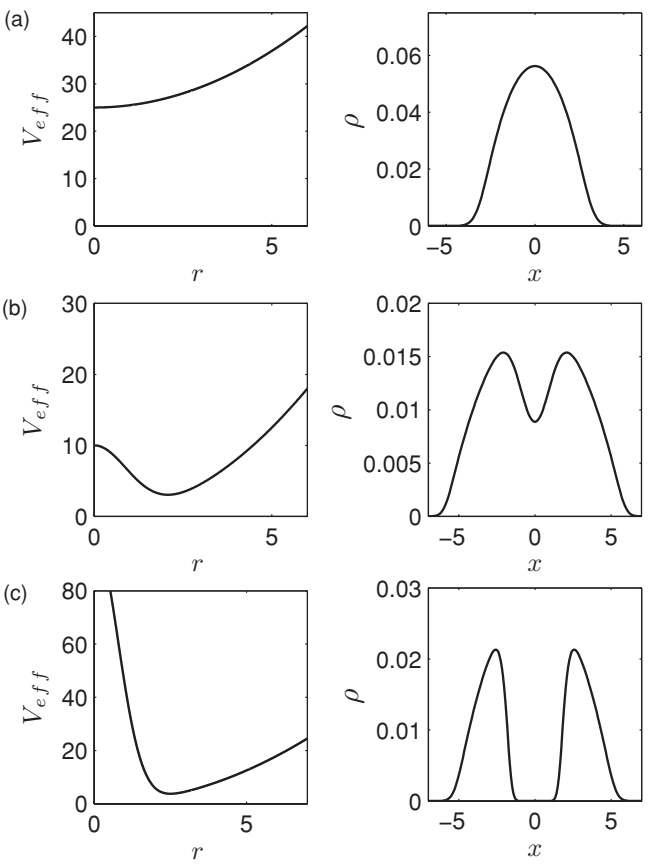

FIG. 1. The effective potential given by Eq. (7) as a function of radial position (left) and the associated density ($\rho = |\psi|^2$) plots taken along $y = 0$ (right). Three parameter sets are considered: (a) $\{g, A, l\} = \{100, 25, 0.03\}$, (b) $\{1000, 10, 0.75\}$, and (c) $\{500, 100, 0.9\}$, all with $\Omega = 0$. Distances are measured in units of $\sqrt{\hbar/(m\omega)}$, density in units of $m\omega/\hbar$, and potentials in units of $\hbar\omega$.

of the condensate, but the condensate is still a disk. The third parameter set displays an inner boundary and the condensate is thus annular.

The effective potential plotted in Fig. 1 only considers a nonrotating condensate, $\Omega = 0$. When the condensate is placed under rotation, vortices form and the shape and size of the condensate are altered. Numerical simulations on the Gross-Pitaevskii equation are carried out to explore the effect of Ω on a range of parameter sets for $\{g, A, l\}$. The two-dimensional, dimensionless, Gross-Pitaevskii equation comes directly from the energy functional (3) and is

$$i\frac{\partial\psi}{\partial t} = -\frac{1}{2}\nabla^2\psi + [V(r) + g|\psi|^2]\psi - i\Omega\left(y\frac{\partial\psi}{\partial x} - x\frac{\partial\psi}{\partial y}\right), \tag{10}$$

for $V(r)$ given by (4). The Gross-Pitaevskii equation is solved numerically in imaginary time (see [21,23]) by evolving an initial wave function for a range of values of $\Omega < 1$ in order to find the ground state. Three cases of interest, which summarize the numerical results well, are presented in the following. The three reported parameter sets are $\{g, A, l\} = \{955.95, 24.83, 0.07\}$, $\{14, 1000, 5\}$, and $\{500, 60, 0.1\}$.

B. The experimental case of Bretin *et al.* [25]

A natural case to numerically simulate is that considered experimentally by Bretin *et al.* [25], where a harmonically trapped condensate is put in rotation with a weak laser beam shone at the origin, modeled by a Gaussian term. This experimental case can be described by a two-dimensional system as explained in the introduction, using the dimensional reduction which leads to the definition of U_0. The experimental values of [25] correspond to $\{g, A, l\} = \{955.95, 24.83, 0.07\}$. A series of contour plots of the density is shown in Fig. 2. (This figure can be compared to the experimental results of [25]: See Fig. 1 of [25], with the appropriate rescaling of rotational velocities, so that the $\Omega^{(2)}_{\rm stir} = 60$ of [25] corresponds to $\Omega = 0.795$ in this paper and $\Omega^{(2)}_{\rm stir} = 69$ corresponds to $\Omega = 0.914$. The rotational velocity is calculated from [25] using the value of the frequency in the x and y direction, $\omega^{(0)}_{\perp}/2\pi = 75.5$ Hz, and not the second stirring phase frequency $\omega_{\perp}/2\pi = 64.8$ Hz.)

For the slow rotational velocities ($\Omega \lesssim 0.5$) of Fig. 2, the condensate is a disk with a small number of vortices [with 12 vortices being present when $\Omega = 0.5$; see Fig. 2(b)] with the vortices forming a triangular lattice. As the rotational velocity is increased, the radius of the outer boundary increases while more vortices are accommodated into the condensate. The dynamics here mimic those observed in harmonic traps.

Above some angular velocity the density at the center of the condensate begins to deplete and eventually an inner boundary (and hence an annulus) is created. In the experiments of [25], a density minimum at the center first occurred for $\Omega \sim 0.874$ (corresponding to $\Omega^{(2)}_{\rm stir} = 66$; see Fig. 1(c) in [25]). The numerical simulations here suggest the onset of the density minimum to be $\Omega \sim 0.887$; see Fig. 2(d) where the density minimum first appears. Clearer pictures of the development of the depletion of density at the center can be seen in Figs. 2(e) and 2(f). The depletion of density distorts the vortex lattice in much the same way that the outer boundary does. In Sec. IV we note that, under the LLL approximation, the vortex lattice inside the central hole is distorted from a regular vortex lattice such that the number of zeros in the hole is given by $R_1 R_2$, to get a number of order R_1^2, where R_1 and R_2 are the inner and outer radii. Increasing the angular velocity still further, thus exploring the fast rotation regime $\Omega \to 1$, details how the density at the center of the condensate continues to diminish until for $\Omega \sim 0.92$ a central hole develops [see Fig. 2(g)] and the condensate becomes annular. The central hole grows rapidly; for $\Omega = 0.93$, the central hole is large and there is a circulation equivalent to 11 vortices [see Fig. 2(h)]. Our simulations have been carried out up to $\Omega \sim 0.95$. These higher angular velocity simulations suggest that both the outer and inner radii and also the width of the condensate increase in size as $\Omega \to 1$.

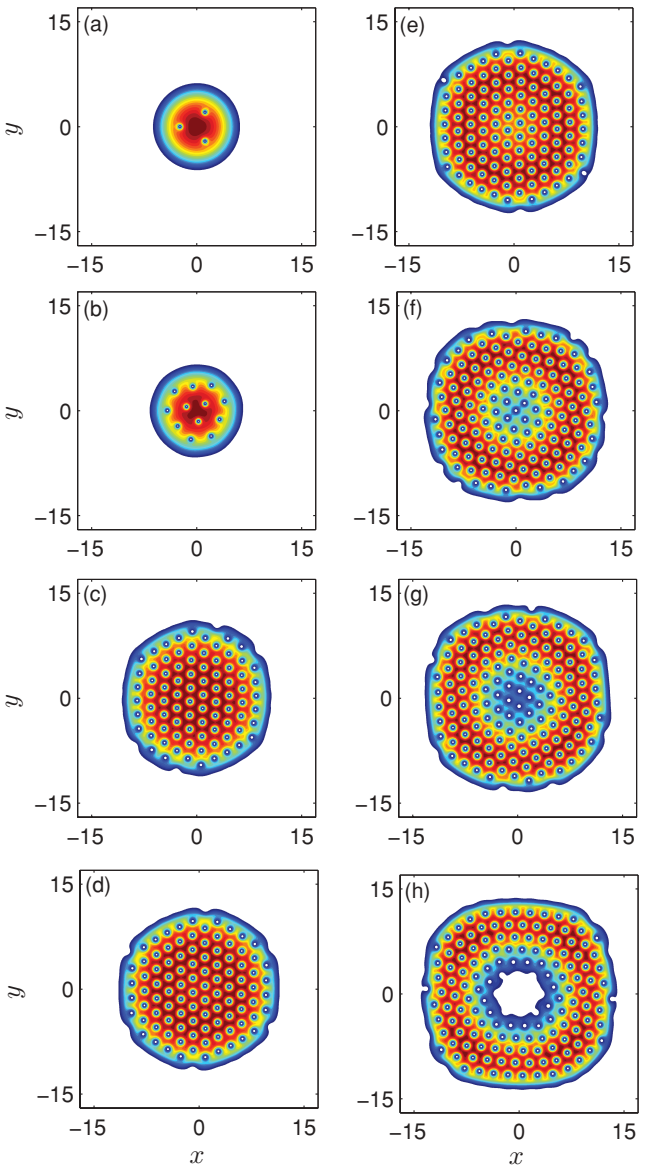

FIG. 2. (Color online) Density profiles of a rotating condensate with $\{g, A, l\} = \{955.95, 24.83, 0.07\}$ corresponding to the (nondimensionalised) experimental values of [25] for (a) $\Omega = 0.25$, (b) $\Omega = 0.5$, (c) $\Omega = 0.874$, (d) $\Omega = 0.887$, (e) $\Omega = 0.901$, (f) $\Omega = 0.914$, (g) $\Omega = 0.92$, and (h) $\Omega = 0.93$. Distances are measured in units of $\sqrt{\hbar/(m\omega)}$.

The experiments of Bretin *et al.* [25] provide an example of the transition from a disk condensate with the density maximum at the center to a disk condensate with a local minimum at the center. It is reasonably safe to assume that if the angular velocity could be further increased in the experiments, the condensate would become annular, with a large persistent current. The depletion of density, which occurs for $\Omega \gtrsim 0.887$, creating a distortion in the vortex lattice and requiring a longer time of convergence for the numerical simulations, must be one of the reasons that explain the experimental difficulties in observing the condensate at these rotation frequencies.

C. The annulus

Manipulating the values of the parameters $\{g, A, l\}$ can have the effect of altering the shape of the condensate. Here we will consider a parameter set that creates an annular condensate that is present for all $\Omega < 1$. The parameter set is thus chosen to be $\{g, A, l\} = \{14, 1000, 5\}$. A selection of contour plots for various angular velocities is given in Fig. 3. The choice of this parameter set is made to illustrate the behavior as Ω gets close to 1.

For low rotational velocities [see Fig. 3(a)], the condensate does not contain vortices in the annulus. However, as Ω approaches unity, both the radius of the inner and outer boundaries increase, but so too does the width of the condensate. When $\Omega = 0.9$ [Fig. 3(b)], the condensate still does not contain any vortices, but for $\Omega = 0.99$ [Fig. 3(c)], the condensate contains two complete rings of vortices. For $\Omega = 0.99$, there is a multiply quantized vortex at the center of the condensate providing a persistent flow with a quantum of circulation $\nu = 3$. The phase profiles also show that there are further singularities of phase ("invisible" vortices) in the outer regions of the condensate.

Note that, for all Ω, the condensate is always an annulus with the inner and outer radii both increasing as Ω increases. Furthermore, the width of the condensate also increases so that a thin annulus is never created. The increase in size of the condensate for $\Omega > 0.9$ is marked. This parameter set explicitly shows the presence, at large Ω, of a central hole containing circulation together with a vortex lattice in the bulk of the condensate.

The choice of this parameter set, especially the value of g, is specifically chosen with reference to the LLL analysis in Sec. IV. As will be noted in Sec. IV, to use the LLL approximation requires $g(1 - \Omega^2)$ to be small. As a consequence, for the numerical simulations to be capable of resolving at Ω close to 1, g must not be too large, though the main features are preserved while increasing g. We note here that an annular condensate, existing at all Ω, can be created for a wide range of values of g.

D. Density dip at the center

As a final numerical example, one can consider the parameter set $\{g, A, l\} = \{500, 60, 0.1\}$. The choice of these parameters actually forces, for $\Omega = 0$, the ground state to have a local nonzero minimum of density at the center. For these parameters the density maximum is located at $r = 4.2$ when $\Omega = 0$ and the condensate is a disk; a contour plot of the condensate at $\Omega = 0$ is given in Fig. 4 along with a selection of other plots for various angular velocities.

Vortices first appear close to the maximum of density instead of close to the center of the condensate. As Ω is increased, the vortex lattice develops close to this initial circle of vortices. The increase in size of the condensate is visible, as is the depletion of density at the center of the condensate, which turns into a hole: An annulus is formed.

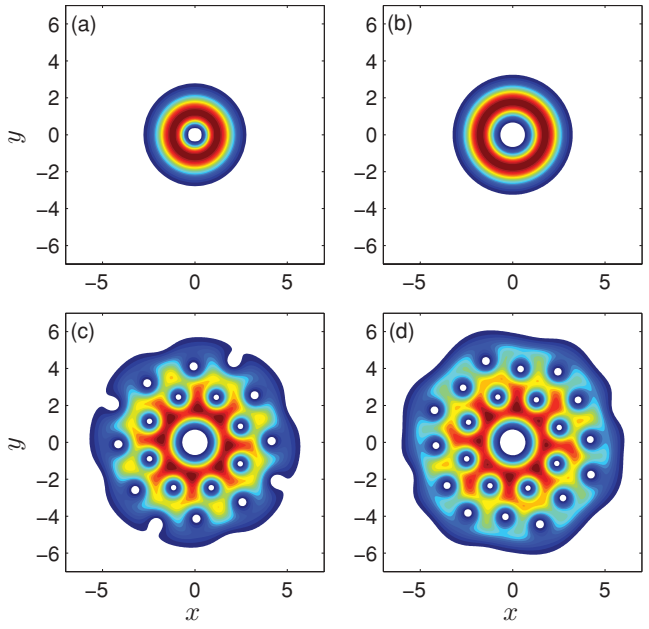

FIG. 3. (Color online) Density profiles of a rotating condensate with $\{g, A, l\} = \{14, 1000, 5\}$ for (a) $\Omega = 0.25$, (b) $\Omega = 0.9$, (c) $\Omega = 0.99$, and (d) $\Omega = 0.994$. Distances are measured in units of $\sqrt{\hbar/(m\omega)}$.

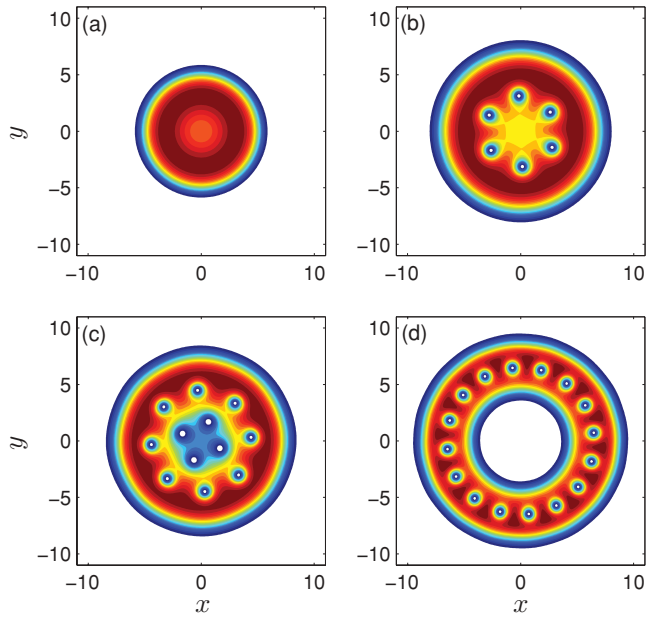

FIG. 4. (Color online) Density profiles of a slow rotating condensate with $\{g, A, l\} = \{500, 60, 0.1\}$ and (a) $\Omega = 0$, (b) $\Omega = 0.225$, (c) $\Omega = 0.35$, and (d) $\Omega = 0.5$. Distances are measured in units of $\sqrt{\hbar/(m\omega)}$.

IV. LOWEST LANDAU LEVEL ANALYSIS

We turn to the analysis of the ground state of the energy (3), where $V(r)$ is given by Eq. (4) and Ω tends to 1. We will use a lowest Landau level analysis [11,17,29]. Recall that the spectrum of the Hamiltonian

$$H_\Omega = -\tfrac{1}{2}\nabla^2 + \tfrac{1}{2}r^2 - \Omega L_z \tag{11}$$

has a Landau level structure. The lowest Landau level is defined as

$$f(x+iy)e^{-\frac{\Omega}{2}(x^2+y^2)}, \quad f \text{ analytic}. \tag{12}$$

For such functions, $\langle H_\Omega\psi, \psi\rangle$ can be simplified (see [17]) so that $E' = \Omega + E_{\mathrm{LLL}}(\psi)$, where

$$E_{\mathrm{LLL}}(\psi) = \int_{\mathcal{V}} \left(V(r) - \frac{1}{2}\Omega^2 r^2\right)|\psi|^2 + \frac{g}{2}|\psi|^4 dV. \tag{13}$$

The minimization of Eq. (13) without the analytic constraint provides the Thomas-Fermi profile for the coarse-grain density:

$$|\psi|^2 = \rho_{\mathrm{TF}} := \lambda - \frac{1}{g}\left(V(r) - \frac{1}{2}\Omega^2 r^2\right). \tag{14}$$

Such a function can be recovered in the LLL by the presence of the vortex lattice and this only changes the coefficient g into bg, where b is the Abrikosov parameter as we explain further in the following.

We recall that the orthogonal projection for a general function ψ onto the LLL is explicit [30,31] and given by

$$\Pi_{\mathrm{LLL}}(\psi) = \frac{1}{\pi}\int e^{-\frac{1}{2}(|z|^2 - 2z\overline{z'} + |z'|^2)}\psi(x', y')dx'dy', \tag{15}$$

where $z = x + iy$ and $z' = x' + iy'$. If an LLL function ψ [i.e., ψ satisfies Eq. (12)] minimizes the energy, Eq. (13), it is a solution of the projected Gross-Pitaevskii equation:

$$\Pi_{\mathrm{LLL}}[(V(r) - \Omega^2 r^2/2 + g|\psi|^2 - \mu)\psi] = 0, \tag{16}$$

where μ is the chemical potential.

When Ω is close to 1, and $V(r)$ is the harmonic plus Gaussian potential, Eq. (16) can be approximated by $\Pi_{\mathrm{LLL}}[g|\psi|^2\psi] = \mu\psi$, which is the equation of the Abrikosov problem (see [11,29,32]). A solution can then be constructed using the theta function (see [29] for the details):

$$\phi(x, y; \tau) = e^{\frac{1}{2}(z^2 - |z|^2)}\Theta\left(\sqrt{\frac{\tau_I}{\pi}}z, \tau\right), \tag{17}$$

where $\tau = \tau_R + i\tau_I$ is the lattice parameter. The zeros of the function ϕ lie on the lattice $\sqrt{\frac{\pi}{\tau_I}}(\mathbb{Z} \oplus \mathbb{Z}\tau)$ and $|\phi|$ is periodic. The optimal lattice, that is, the one minimizing $\mu(\tau) = \int|\phi|^4/(\int|\phi|^2)^2$, is hexagonal, which corresponds to $\tau = e^{2i\pi/3}$ (where the integrals are taken on one period). For $\tau = e^{2i\pi/3}$, $\mu(\tau) = b \sim 1.16$.

As in [29], we can construct an approximate ground state by multiplying the solution, Eq. (17), of the Abrikosov problem by a profile ρ varying on the same scale as ρ_{TF}, which is large. Since this product is not in the LLL, we project it onto the LLL and define $v = \Pi_{\mathrm{LLL}}(\sqrt{\rho(x, y)}\phi(x, y; e^{2i\pi/3}))$. Estimating the energy of v yields

$$E_{\mathrm{LLL}}(v) \sim \int_{\mathbb{R}^2}\left(V(r) - \frac{1}{2}\Omega^2 r^2\right)\rho(x, y) + \frac{gb}{2}\rho(x, y)^2.$$

In this computation it is assumed that ϕ and ρ do not vary on the same scale; hence the integrals can be decoupled. Then, minimizing with respect to ρ implies that ρ must be a Thomas-Fermi profile [Eq. (14)] with g changed into bg:

$$\rho(x, y) = \lambda - \frac{1}{bg}\left(V(r) - \frac{1}{2}\Omega^2 r^2\right). \tag{18}$$

This approximation is valid provided the energy obtained, $E_{\mathrm{LLL}}(v)$, is much smaller than the gap between two Landau levels, which is of the order unity.

In the case of the harmonic potential $V(r) = r^2/2$, the Thomas-Fermi profile provides a disk condensate of radius $R = \{4gb/[\pi(1-\Omega^2)]\}^{1/4}$, which is large when Ω gets close to 1. Moreover, $E_{\mathrm{LLL}}(v)$ is of order $\sqrt{g(1-\Omega^2)}$, which is indeed small when Ω is close to 1 and g is not too large, so that the LLL approximation is satisfied. In the case of the toroidal potential (4), we have to compute the Thomas-Fermi profile from Eq. (18) and discriminate whether it is a disk or an annulus. Then we have to check whether the LLL approximation is justified, that is, whether $E_{\mathrm{LLL}}(v)$ is small.

A. Disk condensate

Suppose that the condensate is a disk (recall that this requires that q is not too large), so that only an outer boundary exists and we write

$$gb|\psi|^2 = \mu + \tfrac{1}{2}(\Omega^2 - 1)r^2 - Ae^{-l^2 r^2}. \tag{19}$$

To find approximations to the radius of the outer boundary one can proceed by taking Eq. (19) and the normalization condition (5), which provide the necessary starting equations in order to compute μ. A check on the validity of the LLL approximation is to verify, in the limit $\Omega \to 1$, that the chemical potential μ is small.

To begin, substitute the density, $|\psi|^2$, from Eq. (19) into the normalization condition (5) and integrate over the domain between 0 and R_2, where R_2 is defined as the radius of the outer boundary. It follows that

$$\frac{gb}{\pi} = \mu R_2^2 + \frac{1}{4}(\Omega^2 - 1)R_2^4 + \frac{A}{l^2}\left(e^{-l^2 R_2^2} - 1\right), \tag{20}$$

which explicitly contains the chemical potential μ. To remove μ from the calculations, one can note from Eq. (19) that

$$\left.\frac{\mu - V_{\mathrm{eff}}(r)}{gb}\right|_{R_2} = |\psi|^2\big|_{R_2} = 0, \tag{21}$$

from which

$$\mu = Ae^{-l^2 R_2^2} - \tfrac{1}{2}(\Omega^2 - 1)R_2^2. \tag{22}$$

Using Eq. (22) in Eq. (20) gives

$$\frac{gb}{\pi} = \frac{1}{4}(1 - \Omega^2)R_2^4 + A\left[R_2^2 e^{-l^2 R_2^2} + \frac{1}{l^2}\left(e^{-l^2 R_2^2} - 1\right)\right]. \tag{23}$$

At this stage we introduce the parameter p, defined as

$$p \equiv \frac{gl^4}{\pi(1-\Omega^2)}. \tag{24}$$

We are interested in the limit Ω close to 1 (i.e., $p \gg 1$), which corresponds to $l^2 R_2^2 \gg 1$. Then the exponential terms in Eq. (23) immediately disappear and it follows that

$$R_2 \sim \left(\frac{4}{(1-\Omega^2)} \left[\frac{gb}{\pi} + \frac{A}{l^2} \right] \right)^{1/4} \tag{25}$$

and

$$\mu \sim \left((1-\Omega^2) \left[\frac{gb}{\pi} + \frac{A}{l^2} \right] \right)^{1/2}. \tag{26}$$

This implies that $l^2 R_2^2$ is large and μ is small since Ω is close to 1. Recall that the assumption of a disk condensate requires q to be bounded, $q < 1+\delta$, and thus (as δ is not large)

$$Al^2 < \frac{(1+\delta)(1-\Omega^2)}{2}, \tag{27}$$

so that the ratio Al^2 has to be small in this regime.

B. Annular condensate

Expressions (25) and (26) are valid strictly when there is no inner boundary, which occurs when $q < 1+\delta$. If $q \geqslant 1+\delta$ then an inner boundary, at $r = R_1$, develops.

One again starts from Eq. (19), but this time the integration is taken over the domain between R_1 and R_2. It then follows that

$$\frac{gb}{\pi} = \mu \left(R_2^2 - R_1^2 \right) + \frac{1}{4}(\Omega^2 - 1) \left(R_2^4 - R_1^4 \right) + \frac{A}{l^2} \left(e^{-l^2 R_2^2} - e^{-l^2 R_1^2} \right), \tag{28}$$

which again explicitly contains the chemical potential μ. To remove μ from the calculations, we note from Eq. (19) that

$$\left. \frac{\mu - V_{\text{eff}}(r)}{gb} \right|_{R_1, R_2} = \left. |\psi|^2 \right|_{R_1, R_2} = 0, \tag{29}$$

from which we recover Eq. (22) and

$$e^{-l^2 R_2^2} - e^{-l^2 R_1^2} = \frac{1}{2A}(\Omega^2 - 1)\left(R_2^2 - R_1^2 \right). \tag{30}$$

Upon substitution of Eq. (22) and Eq. (30) into Eq. (28) and writing the "area" of the annulus as $X \equiv R_2^2 - R_1^2$, we get

$$gb = \frac{1}{2}\pi X(\Omega^2 - 1) \left[\frac{X e^{-l^2 X}}{e^{-l^2 X} - 1} + \frac{1}{l^2} - \frac{X}{2} \right]. \tag{31}$$

Since p is large (because Ω is close to 1), we can assume that $l^2 X$ is large so that the first term in the square brackets of Eq. (31) is negligible, which leaves

$$gb = \frac{1}{2}\pi X^2(\Omega^2 - 1) \left[\frac{1}{l^2 X} - \frac{1}{2} \right]. \tag{32}$$

Now, as $l^2 X$ is taken to be large, one can neglect $1/l^2 X$ in front of the factor of a half in the square brackets. Formally, this corresponds to the following being satisfied:

$$\frac{1}{1-\Omega^2} \gg \frac{\pi}{gl^4}. \tag{33}$$

Thus one obtains an expression for X,

$$X \sim \sqrt{\frac{4gb}{\pi(1-\Omega^2)}}, \tag{34}$$

so that $l^2 X$ is indeed large when Ω gets close to 1. Furthermore, from (30)

$$e^{-l^2 R_1^2} = \frac{(\Omega^2 - 1)X}{2A\left(e^{-l^2 X} - 1\right)}, \tag{35}$$

which, on using the derived approximation for X, Eq. (34), implies that

$$R_1 \sim \frac{1}{l} \left[\ln \left(A \sqrt{\frac{\pi}{gb(1-\Omega^2)}} \right) \right]^{1/2}, \tag{36}$$

giving an expression for the radius of the inner boundary. The value of the chemical potential can then easily be found by taking Eq. (29) evaluated at R_1, with the expression for R_1 following directly from Eq. (36):

$$\mu = \frac{1}{2}(1-\Omega^2)R_1^2 + Ae^{-l^2 R_1^2} \sim \sqrt{\frac{gb(1-\Omega^2)}{\pi}}, \tag{37}$$

provided

$$\ln \left(A \sqrt{\frac{\pi}{gb(1-\Omega^2)}} \right) \ll \left(\frac{4gbl^4}{\pi(1-\Omega^2)} \right)^{1/4}. \tag{38}$$

In the limit $\Omega \to 1$, we see indeed that $\mu \to 0$, thus justifying the LLL approximation provided g is not too large. The radius of the outer boundary can be found by taking Eq. (22) with μ given by (37). Then

$$R_2 \sim \left(\frac{4gb}{\pi(1-\Omega^2)} \right)^{1/4}, \tag{39}$$

which is just $\sqrt{X}$, implicitly implying through (38) that $R_2^2 \gg R_1^2$.

To find the width of the condensate, $d = R_2 - R_1$, it is necessary that R_1 be neglected in front of R_2 (i.e., that $R_1/R_2 \ll 1$), which again is equivalent to Eq. (38) being satisfied. Thus, the width of the condensate d is found from

$$X = (R_2 - R_1)(R_1 + R_2) \Rightarrow d = \frac{X}{R_1 + R_2} \sim \frac{X}{R_2} = \left(\frac{2gb}{\pi(1-\Omega^2)} \right)^{1/4}. \tag{40}$$

Notice that both the width of the condensate d and the inner boundary R_1 and outer boundary R_2 get larger as Ω increases and eventually tend to infinity as $\Omega \to 1$. However, while the width of the condensate and the outer boundary grow like $(1-\Omega^2)^{-1/4}$, the inner boundary grows like $\ln[(1-\Omega^2)^{-1/2}]^{1/2}$. Thus, in the limit $\Omega \to 1$, the condensate forms an infinitely thick annulus with both the inner and outer boundary tending to infinity and with an infinitely large central hole.

TABLE I. A comparison, for parameters $\{g, A, l\} = \{14, 1000, 5\}$, of the values of the inner radius R_1, outer radius R_2, and quantum of circulation ν for fast rotation calculated in the LLL and given by Eqs. (36), (39), and (42), respectively. Numerical values are provided (subscripts n) as a comparison. The chemical potential μ, calculated from Eq. (37), is also given.

Ω	R_1	R_{1n}	R_2	R_{2n}	ν	ν_n	μ
0.9	0.53	0.66	3.23	3.25	1.70	2	0.99
0.99	0.57	0.69	5.68	5.71	3.22	3	0.32
0.994	0.58	0.70	6.45	6.38	3.72	3	0.25

The Cauchy formula allows us to compute the number of zeros $\nu(R_1)$ inside the disk of radius R_1:

$$\nu(R_1) = \frac{R_1 R_2}{2\pi} \int_0^{2\pi} d\theta \frac{\int e^{\frac{R_1}{R_2}\overline{z'}} e^{-|z'|^2} \overline{z'} \sqrt{\rho(z')}\phi(z' e^{-i\theta}, \tau) dz'}{\int e^{\frac{R_1}{R_2}\overline{z'}} e^{-|z'|^2} \sqrt{\rho(z')}\phi(z' e^{-i\theta}, \tau) dz'}, \tag{41}$$

where ϕ comes from (17). Using a Laplace method to evaluate the integrals, we see that, for large R_1, since R_1/R_2 tends to 0,

$$\nu(R_1) \sim R_1 R_2. \tag{42}$$

Note that a regular lattice in a disk of radius R_1 would give $\nu(R_1) \sim R_1^2$, which is much smaller.

C. Summary of the main results

We have derived that, as Ω approaches 1, the condensate has an annular shape with a triangular vortex lattice inside. Equations (36), (39), (37), and (42) provide the inner and outer radii of the condensate, the chemical potential, and the circulation in the inside hole. In the LLL approximation, we must have $\sqrt{g(1-\Omega^2)} \ll 1$. Therefore, in the limit $\Omega \to 1$, the parameter set $\{g, A, l\} = \{14, 1000, 5\}$, described in Sec. IIIC and with a series of contour plots (Fig. 3) showing that the condensate is always annular, satisfies this condition. Table I gives a comparison between the numerical and analytical values for this parameter set and provides a good check on the estimates derived in Eqs. (36), (37), (39), and (42).

V. THOMAS-FERMI APPROXIMATION

In the case of the experiments of Bretin *et al.* [25], Ω is not very close to 1 and g is large, so the LLL analysis of Sec. IV does not adequately describe this experiment. In order to describe it better, and since g is large, we can use the Thomas-Fermi (TF) approximation. In the TF approximation, the vortex cores are a small perturbation with respect to the density profile and yield similar equations to those previously derived in Sec. IV, except that now there is no factor b entering the TF density profile of Eq. (19) since the vortex cores are small. These computations are similar to those in [21]; however, due to the Gaussian trapping potential used here, the condensate becomes a thick annulus, with many vortices, instead of a thin annulus with no vortex as in [21]. This changes significantly the approximations and requires the analysis of several cases according to the magnitude of $l^2 R^2$, with R being the radius of the condensate.

A. Disk condensate

If there is no inner boundary then the Thomas-Fermi approximation leads to

$$g|\psi|^2 = \mu + \tfrac{1}{2}(\Omega^2 - 1)r^2 - A e^{-l^2 r^2}. \tag{43}$$

We substitute the density $|\psi|^2$ from Eq. (43) into the normalization condition (5) and integrate over the domain between 0 and R_2, where as before R_2 is defined as the radius of the outer boundary. It follows that

$$\frac{g}{\pi} = \mu R_2^2 + \frac{1}{4}(\Omega^2 - 1)R_2^4 + \frac{A}{l^2}\left(e^{-l^2 R_2^2} - 1\right), \tag{44}$$

which explicitly contains the chemical potential μ. To remove μ from the calculations, one can note from Eq. (43) that

$$\left.\frac{\mu - V_{\text{eff}}(r)}{g}\right|_{R_2} = |\psi|^2\big|_{R_2} = 0, \tag{45}$$

from which we get

$$\mu = A e^{-l^2 R_2^2} - \tfrac{1}{2}(\Omega^2 - 1)R_2^2, \tag{46}$$

which is the same as (22). Using Eq. (46) in Eq. (44) yields

$$\frac{g}{\pi} = \frac{1}{4}(1 - \Omega^2)R_2^4 + A\left[R_2^2 e^{-l^2 R_2^2} + \frac{1}{l^2}\left(e^{-l^2 R_2^2} - 1\right)\right]. \tag{47}$$

If l is taken to be small as in the experiments, we can assume that p is small and thus that $l^2 R_2^2$ is small. Then the exponentials in $l^2 R_2^2$ can be expanded and it readily follows that

$$p \sim \tfrac{1}{4} l^4 R_2^4 (1 - q) + \tfrac{1}{6} q l^6 R_2^6, \tag{48}$$

where we have used the expressions for q and p [Eqs. (9) and (24), respectively]. Equation (48) is a cubic equation in $l^2 R_2^2$. When $q < 1$, the last term in Eq. (48) can be neglected and we get

$$R_2^4 \sim \frac{4p}{l^4(1-q)} = \frac{4g}{\pi[(1-\Omega^2) - A l^2]}. \tag{49}$$

When q becomes larger than 1, then $1 - q < 0$, but since we assume that we have a disk condensate, we recall that $1 - q$ is small. In such situations, the last term in Eq. (48) cannot be neglected and is crucial to get the correct sign on the right-hand side of (48).

The chemical potential is derived from Eq. (46),

$$\mu \sim A\left(1 - \frac{p}{q}\right) + \frac{1}{2}R_2^2(1 - \Omega^2)(1 - q) + \frac{1}{4q} A l^4 R_2^4 (1 + q), \tag{50}$$

with the value of R_2 obtained from Eq. (48). This allows us to check that $g|\psi(0)|^2 \sim \mu - A$ is large, provided $1 - \Omega^2$ is not too small, g is large, and l is small so that p is small. Hence, this justifies our use here of the TF approximation. This is in particular the case for the parameters

TABLE II. A comparison, for parameters $\{g, A, l\} = \{955.95, 24.83, 0.07\}$, for Ω such that the condensate is a disk. The value of the radius of the condensate for different rotational velocities calculated asymptotically from Eq. (48) under the assumption of the TF approximation and calculated numerically is shown.

Ω	R_2 (asymptotically)	R_2 (numerically)
0.1	6.29	6.18
0.25	6.40	6.19
0.5	6.87	6.70
0.795	8.97	9.00
0.821	9.44	9.49

$\{g, A, l\} = \{955.95, 24.83, 0.07\}$ corresponding to the experiments of [25].

Table II gives a comparison between the numerical values and analytical values [calculated from Eq. (48)] for the boundary of the condensate when the condensate is still a disk ($\Omega \lesssim 0.92$), with the agreement found to be extremely good.

A specific feature of our numerics in the case $\{g, A, l\} = \{500, 60, 0.1\}$ is to find, for certain values of the parameters, since the maximum of the density is not at the origin, that vortices appear on a specific circle rather than at the origin [see Fig. 4(b)]. We call $\rho(r)$ the average of $|\psi|^2$ on a circle of radius r. Then ρ is not far from the TF approximation of $|\psi|^2$ given by (43), but not exactly since the presence of the circle of vortices has an influence on its shape. A computation similar to that in [22] would be required to determine ρ in this setting. Once this is done, one should be able to use the results of [33] (Chap. 3): that the radius where the circle of vortices appears is given by the location where the function ζ/ρ reaches its maximum, where $\zeta(r) = \int_r^R s\rho(s)ds$, with R being the radius of the condensate. This follows from an expansion of the Gross-Pitaevskii energy, where the leading order is given by the energy of vortices of order $\rho(r)\ln\xi$, where ξ is the scattering length, minus the L_z term, which can be estimated as $-\Omega\zeta(r)$. Thus, the lowest Ω for nucleation of vortices is achieved when there is a radius where ζ/ρ is minimal.

B. Annular condensate

When the condensate is an annulus, then in the TF approximation, we need to take into account the quantum of circulation ν in the inner hole of the condensate. We assume that $\psi = |\psi|e^{i\nu S}$, where S is the phase. Note that this is not needed in the LLL approach, because the circulation is incorporated into the LLL wave function and we can compute it directly from (41).

The TF density expression (43) is adjusted to

$$g|\psi|^2 = \tilde{\mu} + \frac{1}{2}\left[(\Omega^2-1)r^2 - \frac{\nu^2}{r^2}\right] - Ae^{-l^2r^2}, \quad (51)$$

where $\tilde{\mu} = \mu + \Omega\nu$. The TF density (51) and the normalization condition (5) provide the starting points from which approximations to the values of the radii of the condensate boundaries and thus the width of the condensate can be found. It follows then that

$$0 = \tilde{\mu} + \frac{1}{2}\left[(\Omega^2-1)r^2 - \frac{\nu^2}{r^2}\right] - Ae^{-l^2r^2}\Big|_{R_1,R_2}, \quad (52)$$

and eliminating $\tilde{\mu}$ from Eq. (52) gives

$$\nu^2 = R_1^2R_2^2\left[(1-\Omega^2) + \frac{2A}{X}e^{-l^2R_1^2}\left(e^{-l^2X}-1\right)\right], \quad (53)$$

where X is the "area" of the condensate and is again defined as $X \equiv R_2^2 - R_1^2$. From integration of the normalization condition (5) between R_1 and R_2 it ensues that

$$\frac{g}{\pi} = \frac{1}{4}(1-\Omega^2)X\left(R_1^2+R_2^2\right) - \frac{1}{2}(1-\Omega^2)R_1^2R_2^2\ln\left(\frac{R_2^2}{R_1^2}\right) + Ae^{-l^2R_1^2}\left(e^{-l^2X}-1\right)\left[R_1^2 + \frac{1}{l^2} - \frac{R_1^2R_2^2}{X}\ln\left(\frac{R_2^2}{R_1^2}\right)\right] + AXe^{-l^2X}e^{-l^2R_1^2}. \quad (54)$$

A further expression that connects the quantum of circulation and the inner and outer radii is readily obtained from the minimization of the free energy per particle, $F = E' - \mu\bar{N}$, where $\bar{N}$ is the number of bosons in the condensate [21]. The following integral identity results:

$$g\Omega = 2\nu\pi\int_{R_1}^{R_2}\frac{1}{r}[g|\psi|^2]dr. \quad (55)$$

Integration of Eq. (55) using Eq. (43), together with the expressions for $\tilde{\mu}$ and ν already given, results in

$$\frac{g\Omega}{\pi\nu} = \left[\frac{1}{2}(1-\Omega^2)\left(R_1^2+R_2^2\right) + Ae^{-l^2R_2^2} + \frac{AR_1^2}{X}e^{-l^2R_1^2}\left(e^{-l^2X}-1\right)\right]\ln\left(\frac{R_2^2}{R_1^2}\right) - X(1-\Omega^2) - Ae^{-l^2R_1^2}\left(e^{-l^2X}-1\right) + 2A\int_{R_1}^{R_2}\frac{1}{r}e^{-l^2r^2}dr. \quad (56)$$

In order to proceed it becomes important to estimate the last integral in Eq. (56) according to the size of l^2r^2. The following sections detail two possible limits.

1. $l^2R_2^2$ small

If $l^2R_2^2$ is assumed to be small, then it follows that $l^2R_1^2$ is small as well. Thus expanding the exponential terms in Eq. (53) up to terms of order $l^6R_2^6$ gives

$$\nu^2 \sim R_1^2R_2^2\left[(1-\Omega^2)(1-q) + Al^4R_2^2\right], \quad (57)$$

where we have assumed that $R_2^2 \gg R_1^2$, which implies that we can write $\exp(-l^2X) \sim \exp(-l^2R_2^2)$. In the case of an annular condensate, we have that $q > 1$, so that the first term in Eq. (57) is negative. Therefore in order for the right-hand side of Eq. (57) to be positive, it is required that

$$l^2R_2^2 > \frac{(q-1)(1-\Omega^2)}{Al^2} = 2\left(1-\frac{1}{q}\right). \quad (58)$$

Expansion of Eq. (54) to order $l^6R_2^6$ (again by assuming that $R_2^2 \gg R_1^2$) results in an expression for R_2:

$$p \sim \frac{1}{4}(1-q)l^4R_2^2\left\{R_2^2\left[1+\frac{ql^2}{(1-q)}\left(\frac{R_2^2}{3}-R_1^2\ln\left(R_2^2\right)\right)\right] - 2R_1^2\ln\left(R_2^2\right)\right\} \sim \frac{l^4R_2^4(1-q)}{4}+\frac{ql^6R_2^6}{6}, \tag{59}$$

where we assume that $R_2^2 \gg R_1^2\ln(R_2^2/R_1^2) \sim R_1^2\ln(R_2^2)$. Notice that (59) is actually the same approximation for R_2 as calculated for the disk condensate in the TF approximation [see Eq. (48)]. Finally, we can consider Eq. (56). Expanding the exponential under the integral in powers of l^2r^2 and simplifying (56) gives

$$\begin{aligned}\frac{g\Omega}{\pi\nu} &\sim \frac{1}{2}(1-\Omega^2)R_2^2\left[\ln\left(R_2^2\right)-2\right] \\ &\quad + A\left[2\ln\left(R_2^2\right)-l^2R_2^2\left(\ln\left(R_2^2\right)+1\right)\right. \\ &\quad \left.+\frac{1}{2}l^4R_2^4\left(\ln\left(R_2^2\right)+\frac{1}{2}\right)\right] \\ &\sim \ln\left(R_2^2\right)\left[\frac{1}{2}(1-\Omega^2)R_2^2(1-q)+2A\right],\end{aligned} \tag{60}$$

where we assume that $\ln(R_2^2/R_1^2) \sim \ln(R_2^2) \gg 1$. It follows that

$$\nu \sim \frac{2g\Omega}{\pi\ln\left(R_2^2\right)}\left[R_2^2(1-\Omega^2)(1-q)+4A\right]^{-1}, \tag{61}$$

and thus the inner radius, R_1, is computed from (57) to be

$$R_1 \sim \frac{\nu}{R_2}\left[(1-\Omega^2)(1-q)+Al^4R_2^2\right]^{-1/2}. \tag{62}$$

There are now three equations [(59), (61), and (62)] for R_2, ν, and R_1 that describe the annular condensate in the TF regime with l^2r^2 small. These provide a comparison to the numerical values corresponding to the parameters of Bretin *et al.* [25]. A comparison for the case of $\Omega = 0.92$ and $\Omega = 0.93$ between the numerics [cf. Figs. 2(g) and 2(h)] and analytical estimates is given in Table III. The TF analytical expressions describing the radii of the inner and outer boundaries are reasonably good. However, the quantum of circulation [Eq. (61)] is not providing a suitable estimate. Indeed ν is still small and the inconsistency could be as a result of the difficulty in numerically discriminating between vortices inside the condensate and inside the inner boundary.

TABLE III. A comparison, for parameters $\{g, A, l\} = \{955.95, 24.83, 0.07\}$, for Ω such that the condensate is an annulus. The values of the inner radius R_1, outer radius R_2, and quantum of circulation ν are calculated by a TF analysis and are given by Eqs. (62), (59), and (61), respectively. Numerical values are provided (subscripts n) as a comparison.

Ω	R_1	R_{1n}	R_2	R_{2n}	ν	ν_n
0.92	1.00	0.00	12.94	13.30	1.30	0
0.93	3.72	3.25	13.52	13.80	1.37	11

We note that the Thomas-Fermi approximation is justified because the maximum of $g|\psi|^2$ is larger than 1 (numerically around 4). Larger values of Ω which are not reached by the experiments would be better described by a LLL regime. Nevertheless, in the TF approximation, we can still analyze an intermediate case.

2. $l^2R_1^2$ small and $l^2R_2^2$ large

If we take $l^2R_1^2$ small and $l^2R_2^2$ large then this implies that l^2X is also large. Taking Eqs. (53), (54), and (56) as the starting point we note immediately that (53) simplifies to

$$\nu^2 = R_1^2R_2^2(1-\Omega^2), \tag{63}$$

while Eq. (54) simplifies to

$$\begin{aligned}\frac{g}{\pi} &\sim \frac{1}{4}(1-\Omega^2)R_2^4-\frac{1}{2}(1-\Omega^2)R_1^2R_2^2\ln\left(R_2^2\right) \\ &\quad - Ae^{-l^2R_1^2}\left[R_1^2+\frac{1}{l^2}\right] \\ &\sim \frac{1}{4}(1-\Omega^2)R_2^2\left[R_2^2-2R_1^2\ln\left(R_2^2\right)\right]-AR_1^2\left(1+\frac{1}{l^2R_1^2}\right) \\ &\sim \frac{1}{4}(1-\Omega^2)R_2^4-\frac{A}{l^2},\end{aligned} \tag{64}$$

where we have assumed that

$$R_2^2 \gg R_1^2,$$
$$R_2^2 \gg 2R_1^2\ln\left(R_2^2\right),$$

the first condition following directly from the assumption that $l^2R_1^2$ is small and $l^2R_2^2$ is large. Furthermore, Eq. (56) simplifies as

$$\begin{aligned}\frac{g\Omega}{\pi\nu} &\sim \left[\frac{1}{2}(1-\Omega^2)R_2^2-\frac{2AR_1^2}{X}\right]\ln\left(R_2^2\right)-R_2^2(1-\Omega^2) \\ &\quad + A+\frac{A}{e}-2A\ln(lR_1)-\frac{A}{l^2R_2^2}e^{-l^2R_2^2} \\ &\sim \frac{1}{2}(1-\Omega^2)R_2^2\left[\ln\left(R_2^2\right)-2\right] \\ &\sim \frac{1}{2}(1-\Omega^2)R_2^2\ln\left(R_2^2\right),\end{aligned} \tag{65}$$

since

$$\int_{R_1}^{R_2}\frac{1}{r}e^{-l^2r^2}dr \sim -\ln(lR_1)+\frac{1}{2e}-\frac{1}{2l^2R_2^2}e^{-l^2R_2^2}, \tag{66}$$

in the limits $l^2R_1^2$ small and $l^2R_2^2$ large. Thus we get an expression for the outer boundary, from Eq. (64), as

$$R_2 \sim \left[\frac{4}{(1-\Omega^2)}\left(\frac{g}{\pi}+\frac{A}{l^2}\right)\right]^{1/4}, \tag{67}$$

and from Eq. (65) we get an expression for the quantum of circulation,

$$\nu \sim \frac{2g\Omega}{\pi(1-\Omega^2)R_2^2\ln\left(R_2^2\right)}, \tag{68}$$

with R_2 found from Eq. (67). Notice how the value of ν gets large in the limit $\Omega \to 1$. Putting Eqs. (67) and (68) into

Eq. (63) we arrive at the expression for the inner boundary:

$$R_1 \sim \frac{g\Omega R_2}{2\pi \ln\left(R_2^2\right)}\left[(1-\Omega^2)^{1/2}\left(\frac{g}{\pi}+\frac{A}{l^2}\right)\right]^{-1}, \quad (69)$$

again for R_2 given by Eq. (67).

Such a case is not reached experimentally and is just before the LLL regime. One could perform similar computations assuming that $l^2 R_1^2$ is also large.

VI. CONCLUSION

Motivated by the experiments of [25], we provide numerical and analytical computations which describe the properties of a condensate placed in a harmonic plus Gaussian trap. We have seen that, however close Ω gets to the harmonic trapping frequency, the condensate becomes a large annulus containing a triangular vortex lattice, contrary to what is seen for a condensate with a quadratic plus quartic term where the width of the condensate decreases. We estimate the circulation in the central hole, which is higher than that corresponding to a regular lattice in this region. Also in a Thomas-Fermi approximation, when the rotational velocity Ω is not too close to the harmonic trapping frequency, we estimate the radii of the condensate and the circulation in the inside hole, in a way which is consistent with numerics.

ACKNOWLEDGMENTS

We acknowledge support from the French ministry Grant ANR-BLAN-0238, VoLQuan.

[1] E. M. Lifshitz and L. P. Pitaevskii, *Statistical Physics, Part 2* (Butterworth-Heinemann, London, 1980), Chap III.
[2] R. J. Donnelly, *Quantized Vortices in Helium II* (Cambridge University Press, Cambridge, 1991), Chaps. 4 and 5.
[3] M. R. Matthews, B. P. Anderson, P. C. Haljan, D. S. Hall, C. E. Wieman, and E. A. Cornell, Phys. Rev. Lett. **83**, 2498 (1999).
[4] K. W. Madison, F. Chevy, W. Wohlleben, and J. Dalibard, Phys. Rev. Lett. **84**, 806 (2000).
[5] A. L. Fetter, Phys. Rev. A **75**, 013620 (2007).
[6] A. L. Fetter, Rev. Mod. Phys **81**, 647 (2009).
[7] J. R. Abo-Shaeer, C. Raman, J. M. Vogels, and W. Ketterle, Science **292**, 476 (2001); C. Raman, J. R. Abo-Shaeer, J. M. Vogels, K. Xu, and W. Ketterle, Phys. Rev. Lett. **87**, 210402 (2001).
[8] P. Engels, I. Coddington, P. C. Haljan, V. Schweikhard, and E. A. Cornell, Phys. Rev. Lett. **90**, 170405 (2003).
[9] V. Schweikhard, I. Coddington, P. Engels, V. P. Mogendorff, and E. A. Cornell, Phys. Rev. Lett. **92**, 040404 (2004).
[10] I. Coddington, P. C. Haljan, P. Engels, V. Schweikhard, S. Tung, and E. A. Cornell, Phys. Rev. A **70**, 063607 (2004).
[11] T. L. Ho, Phys. Rev. Lett. **87**, 060403 (2001).
[12] N. R. Cooper, Adv. Phys. **57**, 539 (2008).
[13] G. Baym and C. J. Pethick, Phys. Rev. A **69**, 043619 (2004).
[14] G. Watanabe, G. Baym, and C. J. Pethick, Phys. Rev. Lett. **93**, 190401 (2004).
[15] N. R. Cooper, S. Komineas, and N. Read, Phys. Rev. A **70**, 033604 (2004).
[16] U. R. Fischer and G. Baym, Phys. Rev. Lett. **90**, 140402 (2003).
[17] A. Aftalion, X. Blanc, and J. Dalibard, Phys. Rev. A **71**, 023611 (2005).
[18] K. Kasamatsu, M. Tsubota, and M. Ueda, Phys. Rev. A **66**, 053606 (2002).
[19] A. Aftalion and I. Danaila, Phys. Rev. A **69**, 033608 (2004).
[20] J. K. Kim and A. L. Fetter, Phys. Rev. A **72**, 023619 (2005).
[21] A. L. Fetter, B. Jackson, and S. Stringari, Phys. Rev. A **71**, 013605 (2005).
[22] H. Fu and E. Zaremba, Phys. Rev. A **73**, 013614 (2006).
[23] M. Cozzini, B. Jackson, and S. Stringari, Phys. Rev. A **73**, 013603 (2006).
[24] X. Blanc and N. Rougerie, Phys. Rev. A **77**, 053615 (2008).
[25] V. Bretin, S. Stock, Y. Seurin, and J. Dalibard, Phys. Rev. Lett. **92**, 050403 (2004).
[26] S. Stock, V. Bretin, F. Chevy, and J. Dalibard, Europhys. Lett. **65**, 594 (2004).
[27] C. Ryu, M. F. Andersen, P. Clade, V. Natarajan, K. Helmerson, and W. D. Phillips, Phys. Rev. Lett. **99**, 260401 (2007).
[28] C. N. Weiler *et al.*, Nature (London) **455**, 948 (2008).
[29] A. Aftalion, X. Blanc, and F. Nier, Phys. Rev. A **73**, 011601(R) (2006).
[30] V. Bargmann, Commun. Pure Appl. Math. **14**, 187 (1961).
[31] S. M. Girvin and T. Jach, Phys. Rev. B **29**, 5617 (1984).
[32] A. A. Abrikosov, Zh. Eksp. Teor. Fiz. **32**, 1442 (1957); W. H. Kleiner, L. M. Roth, and S. H. Autler, Phys. Rev. **133**, A1226 (1964).
[33] A. Aftalion, *Vortices in Bose-Einstein Condensates* (Birkhauser, Basel, 2006).